Hidden Topological Structure of Flow Network Functionality

Jason W. Rocks, Andrea J. Liu,* and Eleni Katifori
Department of Physics and Astronomy, University of Pennsylvania, Philadelphia, Pennsylvania 19104, USA

(Received 13 December 2019; revised 1 July 2020; accepted 29 October 2020; published 13 January 2021)

The ability to reroute and control flow is vital to the function of venation networks across a wide range of organisms. By modifying individual edges in these networks, either by adjusting edge conductances or creating and destroying edges, organisms robustly control the propagation of inputs to perform specific tasks. However, a fundamental disconnect exists between the structure and function: networks with different local architectures can perform the same functions. Here, we answer the question of how changes at the level of individual edges collectively create functionality at the scale of an entire network. Using persistent homology, we analyze networks tuned to perform complex tasks. We find that the responses of such networks encode a hidden topological structure composed of sectors of nearly uniform pressure. Although these sectors are not apparent in the underlying network structure, they correlate strongly with the tuned function. The connectivity of these sectors, rather than that of individual nodes, provides a quantitative relationship between structure and function in flow networks.

DOI: 10.1103/PhysRevLett.126.028102

The ability to control the transport of materials between distant sites is central to the function of many biological flow networks. Often, the rerouting of fluid flow can be controlled on demand as dictated by the needs of the system. By dynamically contracting and dilating blood vessels, the cerebral vasculature actively controls blood flow to support local neuronal activity throughout the brain [1,2]; impairment of this ability has been linked to neurological diseases [3,4]. More generally, the ability to tune edge conductances or locally restructure node connectivity enables animals [5,6], plants [7,8], fungi [9], and slime molds [10] to regulate flow through the network to deliver or take up water, nutrients, oxygen, and metabolic byproducts as needed.

While vascular networks of individuals within a species —and sometimes between related species—often share common macroscale and mesoscale network architectures, local (microscale) network structures often differ, lacking an established underlying geometric organizational principle [11]. In spite of this structural variation, different networks manipulate local structure to achieve the same basic tasks. How do vascular networks with different local structures manage to redirect flow to perform the same collective functions? What is the relationship between structure and function in this context?

To answer these questions, we first observe that all biological flow networks that tune themselves to reroute flow must satisfy two classes of physical constraints. First, all tuning processes are accompanied by changes in the pressure response to external (or internal) stimuli. Whether a system is aiming to achieve specific localized flow rates (current), maintain perfusion of flow, etc., changes in node pressures or pressure drops across edges in the network must occur, even if they are not the direct means of control. To linear order, pressure is controlled by a combination of Darcy's Law and conservation of mass, resulting in a discrete Laplace's equation which imposes constraints that must be satisfied by any flow network.

Second, any task associated with rerouting flow requires controlling pressure (e.g., enhancing local flow, as just discussed) at "target" sites in the network in response to pressure (associated with incoming or outgoing flow) at a "source" elsewhere in the network. There is a descriptive and mathematical similarity between the task of controlling flow at a target in response to a pressure source and the task, known as "allostery," of controlling binding of a molecule at some location on a protein by binding a second molecule at a distant source site on the protein. We therefore refer to functions associated with regulating flow at target sites in response to distant sources as "flow allostery." While the details of specific biological systems and tasks can impose additional constraints on a system, the constraints imposed by flow allostery must be present.

To explore the effects of these two classes of constraints in the context of flow transport, we create networks that perform flow allostery in which we directly control the target pressure response. We appeal to the "tuning-by-pruning" framework [12–15], in which flow networks are tuned to perform highly complex multifunctional tasks; by selectively tuning the conductances of a small fraction of edges, the pressure differences at many of prespecified target edges can be simultaneously controlled in response to a pressure source applied elsewhere in the system. Such edge-based allosteric functions are quite general since any pressure response can be decomposed into a collection of dipoles.

In analogy to biological vascular systems, different networks in this framework can easily be tuned to develop the same function (i.e., the same number of target edges and desired target pressure differences), yielding *ensembles* of networks with the same collective functions. Instead of being restricted to limited data collected from experiments, we generate statistically large numbers of realizations, allowing us to discern even weak signatures of allosteric function and to draw conclusions with high confidence. Here, we use this approach to develop an analysis of tuned network ensembles that reveals the local structure governing allosteric function in flow networks.

To identify the underlying basis of allosteric function in flow networks, we apply persistent homology to tuned network ensembles. We find that the structure-function relationship is topologically encoded in the response: as a network is tuned to achieve a desired target pressure difference at a number of different sites, it separates into sectors of relatively uniform node pressure. It is the connectivity, or topology, of these *sectors* that determines the function, rather than the connectivity of the actual nodes. Our finding provides a simple, unifying topological description of all networks tuned for the same function, regardless of the underlying network architecture, along with the quantitative means to compare networks tuned for different functions. This description is robust even when the magnitude of the tuned response is small and the sectors cannot be identified by eye. Moreover, our analysis is general so it can potentially be applied to experimental data on real systems.

To create ensembles of flow networks that each perform the same allosteric functions, we first generate a collection of networks and then tune each one by adjusting edge conductances [15]. Specifically, we consider flow networks (or equivalently, resistor networks) in which edges between nodes represent pipes (linear resistors). The network's response to external stimuli, described by the node pressures (voltages), is governed by a discrete Laplace's equation equivalent to Kirchoff's laws. We use contact networks of randomly generated two and three-dimensional packings of soft spheres with periodic boundary conditions, created using standard jamming algorithms. To convert to a flow network, we assign a conductance to each edge, chosen randomly between 0.1 to 1.0 in discrete increments of 0.1.

We next tune each flow network to perform a specific function, so that the pressure differences of specified target edges must exceed $\Delta > 0$ when a unit pressure difference is applied across a specified source edge. For each network, the source and target edges are chosen randomly with the constraint that they do not share any nodes. To achieve a target pressure difference $\Delta p_T \geq \Delta$ across each target, we use a greedy algorithm: in each step we increase or decrease the conductance of a single edge by 0.1 (staying within [0, 1], inclusively), modifying the edge conductance that best optimizes the total response at that step (for further details see Refs. [15,16], as well as Ref. [13] for mechanical networks). Tuning algorithm details do not affect the generality of our results [15].

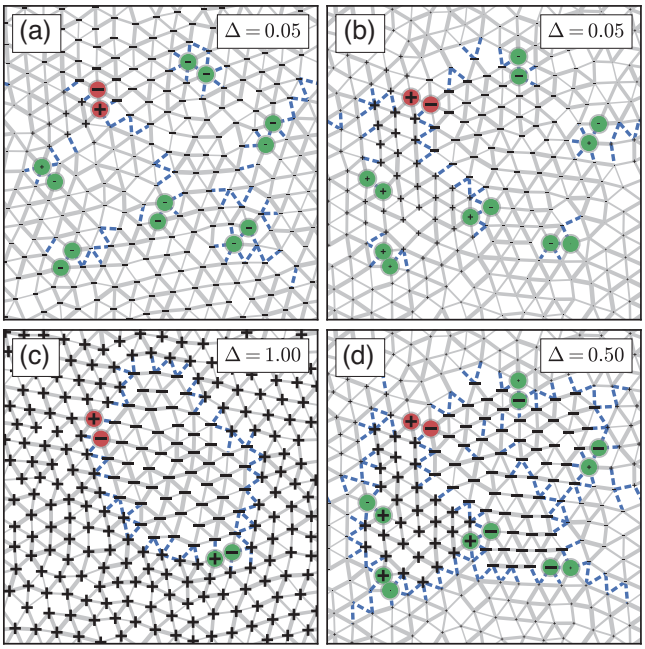

FIG. 1. (a),(b) Two different two-dimensional flow networks that perform the same allosteric functions: six target node pairs (green), respond with a pressure difference of $\Delta p_T \geq 0.05$ to a unit pressure difference between two source nodes (red). The sign of the node pressure is in black with size denoting magnitude. Edge conductance is indicated by thickness, with dashed blue lines for edges removed (zero conductance) by tuning. (c) A network with a single function tuned to a maximum pressure difference of $\Delta = 1.0$. (d) The network in (b) tuned to $\Delta p_T \geq 0.5$.

Figures 1(a) and 1(b) illustrate the discrepancy between network structure and function. Two different networks perform the same task: six target edges each have pressure differences $\Delta p_T \geq \Delta$ where $\Delta = 0.05$ relative to the source (we also chose similar relative positions of source and targets for visual clarity). Clearly, the spatial distributions of edge conductances (indicated by edge thickness) and node pressures (indicated by the size of the symbols showing the sign) are different; it is unclear from Figs. 1(a) and 1(b) whether the underlying structures of the two tuned networks share anything in common.

We gain insight by tuning targets to extreme pressure differences. Figure 1(c) displays a network with a single target tuned to the extreme limit $\Delta = 1$, the maximum achievable pressure difference at a target edge. The network clearly separates into two distinct sectors of perfectly uniform node pressure, connected only by a single edge between the source nodes. These two sectors are separated by a cracklike structure with pressure differences of precisely 1.0 across edges removed during the tuning (denoted by dashed blue lines). Similarly, Fig. 1(d) displays

the network from Fig. 1(b), but with each target edge tuned to $\Delta p_T \geq 0.50$. Here, the network separates into three distinct sectors, each of almost perfectly uniform pressure. The exact details of the local structure (which specific edges are modified) do not matter as long as the network partitions into separated connected components with almost all edges connecting the different sectors removed.

In these extreme cases, the relationship between structure and function is clear: the increase in the number of connected components is directly tied to the function. The emergence of sectors represents a topological change in the overall network connectivity beyond that of the local edge structure. Clearly, this description extends to all networks tuned to this extreme limit.

For smaller Δ, as in Figs. 1(a) and 1(b), the entire network remains highly interconnected; there is only one connected component even after the desired function is achieved. The challenge is therefore to apply the insight gained from the extreme case to smaller minimum target pressure differences Δ. In the extreme case, the signature of tuning is not only encoded in the number of connected components but also in the sectors. We therefore turn to topological data analysis to determine whether analogous sectors exist for networks tuned to smaller Δ.

Persistent homology analysis [17,18] discerns topological features in topologically and/or geometrically structured data. This technique provides a systematic means of identifying features at all scales encoded in a function (the pressure response) defined in some space (the network). Each feature we identify corresponds to a region of relatively small pressure differences (relatively uniform node pressures) on the edges in the network. However, many of these regions owe their existence to small spatial fluctuations in the pressure response, and their importance to the function is unclear. This is where persistent homology provides a second benefit: each identified feature is assigned a measure of significance, called *persistence*. We use these persistence values to perform topological coarse graining (a form of hierarchical clustering), combining as many of the lowest persistence regions with their neighbors as possible to achieve the smallest number of sectors. Since the functions we tune into the networks require creating pressure differences between each pair of target nodes, we avoid combining regions that would place both nodes comprising a single target edge into the same sector (details in Ref. [16]). This analysis results in sectors that are minimal and as significant as possible.

Figures 2(a)–2(d) show how the resulting sectors evolve with Δ for the case of a single target, while Figs. 2(e)–2(h) show the same for a multifunctional network. The networks segregate into multiple sectors (two and four, respectively), each composed of nodes with relatively uniform pressures. Figure 2 also depicts histograms of the node pressures for each network, colored according to their corresponding sectors. Depicted above each histogram is a schematic of the connectivity between sectors, representing the coarse-grained topology of each network.

The identified sectors characterize the tuned function quantitatively. To show this, we measure the median node pressure $\bar{p}$ of each sector, shown as vertical dashed lines in the histograms in Fig. 2. For any pair of sectors, we can measure the difference in these median node pressures, which we call the sector pressure difference $\Delta\bar{p}$. We observe that the value of $\Delta\bar{p}$ measured between a pair of sectors corresponding to neighboring peaks in a histogram often corresponds closely to the desired target pressure difference Δ. Therefore, for each pair of target nodes, we measure $\Delta\bar{p}$ between their corresponding sectors and compare this value to the actual pressure difference between the target nodes Δp_T tuned to satisfy $\Delta p_T \geq \Delta$. Figure 3 shows the correlation between $\Delta\bar{p}$ and Δp_T for each target for networks with various numbers of nodes N and targets N_T, for three-dimensional networks (results for two-dimensional networks are presented in Ref. [16]). On average, $\Delta\bar{p}$ is almost perfectly correlated with Δp_T for every system size and number of targets. For larger networks and/or smaller numbers of targets the spread of the distributions around each point (standard deviation indicated by error bars) is extremely small. In the Supplemental Material, we also provide examples of networks designed with alternative tuning strategies (e.g., tuning current rather than pressure difference) [19]. Each of these exhibits the same characteristic sectors, demonstrating that the sector description applies independent of the precise details of tuning.

In summary, we have established the physical origin of function in allosteric flow networks using persistent homology. When a network is tuned to have a desired minimum pressure difference at a collection of targets, it attempts to create flow bottlenecks, individually partitioning each pair of target nodes into separate sectors. The difference in median pressure between two adjacent sectors correlates strongly with the response of target edges spanning them. Therefore, sectors are not only the most topologically significant network features (with large persistence), but also dominate the functional properties. Less topologically significant features, such as fluctuations of node pressures about the mean of each sector, have weaker effects on function.

This sector-based picture provides a unifying description for all flow networks tuned to perform allosteric functions. Although the local node connectivity and geometrical structure can differ between networks tuned for the same function, their commonality in structure encapsulated by the sector connectivity becomes apparent when viewed through a topological lens. This leads us to propose a refinement of the structure-function paradigm in the context of functional flow networks: it is the relationship between the topological structure of the response and

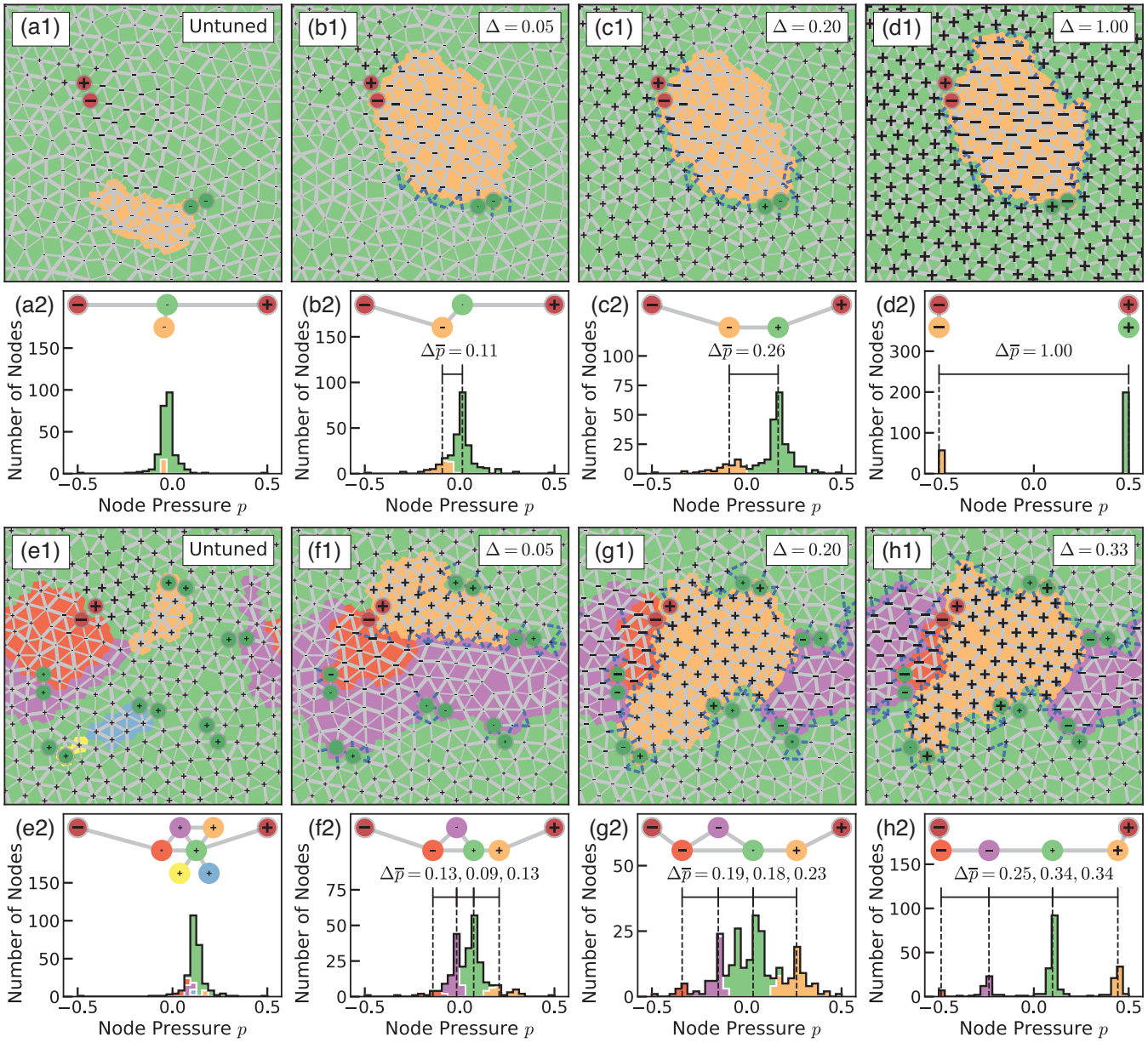

FIG. 2. Topological structure of the response for the network of Fig. 1(c) with a single target (a) before tuning and tuned for target pressure differences of (b) $\Delta p_T \geq \Delta$ where $\Delta = 0.05$, (c) $\Delta p_T \geq 0.2$, and (d) $\Delta p_T \geq 1.0$. Similarly, a multifunctional network with six separate targets (e) before tuning and tuned for (f) $\Delta p_T \geq 0.05$ (g) $\Delta p_T \geq 0.2$, and (h) $\Delta p_T \geq 0.33$. First and third rows: sectors characterizing the response are highlighted by color. Symbols and edges are defined as in Fig. 1. Second and fourth rows: histograms of node pressures colored to indicate contributions from nodes in the corresponding sectors in the networks above. The median node pressure $\bar{p}$ of each sector is shown as a vertical dashed line and differences in median pressures $\Delta\bar{p}$ corresponding to neighboring peaks in the histograms are indicated. The inset in each histogram is a schematic depicting the connectivity between sectors, represented as nodes, with source nodes in red. Edges indicate the existence of edges between sectors in tuned network. Symbols (and approximate horizontal position) denote sign and magnitude of $\bar{p}$.

function that is important. The sector picture also gives insight into the limit of multifunctionality in allosteric networks, corresponding to a transition [15] from a regime in which the response of each target can always be satisfied to one in which not all responses can be satisfied, and is related to the upper bound on the number of sectors (see Supporting Information [19]).

Finally, our analysis suggests a new way to characterize vascular networks. Obtaining an accurate, complete map of every vessel of an entire organ or organism poses a difficult experimental challenge as vascular networks frequently consist of millions of nodes, spanning a range of length scales. Our work shows that this complete map may not always be necessary; sampling local node pressures on

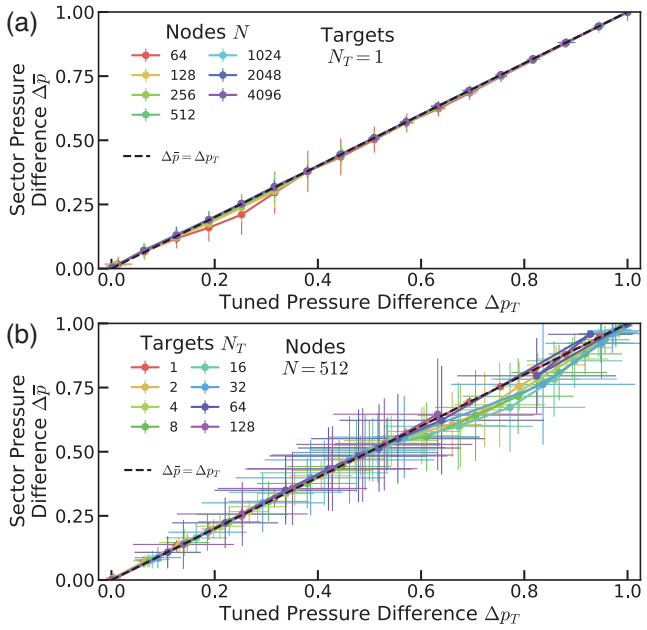

FIG. 3. Correlation of pressure difference between sectors $\Delta\bar{p}$ and tuned pressure difference of target edges Δp_T for 3D networks (a) as a function of the number of nodes N for a single target $N_T = 1$ and (b) at $N = 512$ for various N_T. Both Δp_T and $\Delta\bar{p}$ for each point are averaged over all targets for up to 256 independent networks tuned to the same Δ. Error bars represent standard deviations. The diagonal black dashed lines indicate perfect correlation, $\Delta\bar{p} = \Delta p_T$.

coarser scales may be more useful for characterizing function and be less susceptible to error. An approximate reconstruction of the network (e.g., by assigning edges between nodes below some cutoff length) would likely suffice to perform topological coarse graining and confirm our results. However, thanks to recent experimental advances, high-quality vasculature data from whole mouse brains across all length scales is becoming increasingly available [20,21], suggesting an edge-based approach may be feasible. In principle, one could measure both the rate of blood flow (current) and the diameter (conductance) of each vessel from such images and infer pressure differences via Ohm's law on an edge-by-edge basis. It would then be possible to test whether the correlations and patterns of the pressure differences are consistent with our sector description.

We thank R. D. Kamien and S. R. Nagel for instructive discussions. This research was supported by the NSF through DMR-1506625 (J. W. R.) and PHY-1554887 (E. K.), the Simons Foundation through 454945 (J. W. R. and A. J. L.), 327939 (A. J. L.), and 568888 (E. K.), and the Burroughs Welcome Career Award (E. K.).

*Corresponding author.
ajliu@upenn.edu

[1] M. J. Cipolla, *The Cerebral Circulation*, 2nd ed., edited by D. N. Granger and J. Granger (Morgan & Claypool Publishers, 2016), https://www.morganclaypool.com/doi/abs/10.4199/C00141ED2V01Y201607ISP066.
[2] Y.-R. Gao, S. E. Greene, and P. J. Drew, Mechanical restriction of intracortical vessel dilation by brain tissue sculpts the hemodynamic response, NeuroImage **115**, 162 (2015).
[3] M. D. Sweeney, K. Kisler, A. Montagne, A. W. Toga, and B. V. Zlokovic, The role of brain vasculature in neurodegenerative disorders, Nat. Neurosci. **21**, 1318 (2018).
[4] A. Liesz, The vascular side of Alzheimer's disease, Science **365**, 223 (2019).
[5] R. F. Tuma, W. N. Durán, and K. Ley, *Handbook of Physiology: Microcirculation* (Academic Press, San Diego, 2008).
[6] F. J. Meigel, P. Cha, M. P. Brenner, and K. Alim, Robust Increase in Supply by Vessel Dilation in Globally Coupled Microvasculature, Phys. Rev. Lett. **123**, 228103 (2019).
[7] J. Pitterman, The evolution of water transport in plants: an integrated approach, Geobiology **8**, 112 (2010).
[8] L. Sack and C. Scoffoni, Leaf venation: structure, function, development, evolution, ecology and applications in the past, present and future, New Phytol. **198**, 983 (2013).
[9] L. Heaton, B. Obara, V. Grau, N. Jones, T. Nakagaki, L. Boddy, and M. D. Fricker, Analysis of fungal networks, Fungal Biol. Rev. **26**, 12 (2012).
[10] A. Tero, K. Yumiki, R. Kobayashi, T. Saigusa, and T. Nakagaki, Flow-network adaptation in Physarum amoebae, Theory Biosci. **27**, 89 (2008).
[11] C. Hadjistassou, A. Bejan, and Y. Ventikos, Cerebral oxygenation and optimal vascular brain organization, J. R. Soc. Interface **12**, 20150245 (2015).
[12] C. P. Goodrich, A. J. Liu, and S. R. Nagel, The Principle of Independent Bond-Level Response: Tuning by Pruning to Exploit Disorder for Global Behavior, Phys. Rev. Lett. **114**, 225501 (2015).
[13] J. W. Rocks, N. Pashine, I. Bischofberger, C. P. Goodrich, A. J. Liu, and S. R. Nagel, Designing allostery-inspired response in mechanical networks, Proc. Natl. Acad. Sci. U.S.A. **114**, 2520 (2017).
[14] D. Hexner, A. J. Liu, and S. R. Nagel, Role of local response in manipulating the elastic properties of disordered solids by bond removal, Soft Matter **14**, 312 (2018).
[15] J. W. Rocks, H. Ronellenfitsch, A. J. Liu, S. R. Nagel, and E. Katifori, Limits of multifunctionality in tunable networks, Proc. Natl. Acad. Sci. U.S.A. **116**, 2506 (2019).
[16] J. W. Rocks, A. J. Liu, and E. Katifori, Revealing structure-function relationships in functional flow networks via persistent homology, Phys. Rev. Research **2**, 033234 (2020).
[17] H. Edelsbrunner and J. L. Harer, in *Computational Topology: An Introduction* (American Mathematical Society, Providence, 2010).
[18] N. Otter, M. A. Porter, U. Tillmann, P. Grindrod, and H. A. Harrington, A roadmap for the computation of persistent homology, EPJ Data Sci. **6**, 17 (2017).
[19] See Supplemental Material at http://link.aps.org/supplemental/10.1103/PhysRevLett.126.028102 for networks designed with alternative tuning strategies and results regarding the limits of multifunctionality.

[20] A. P. Di Giovanna, A. Tibo, L. Silvestri, M. C. Müllenbroich, I. Costantini, A. L. A. Mascaro, L. Sacconi, P. Frasconi, and F. S. Pavone, Whole-brain vasculature reconstruction at the single capillary level, Sci. Rep. **8**, 12573 (2018).

[21] C. Kirst, S. Skriabine, A. Vieites-Prado, T. Topilko, P. Bertin, G. Gerschenfeld, F. Verny, P. Topilko, N. Michalski, M. Tessier-Lavigne, and N. Renier, Mapping the fine-scale organization and plasticity of the brain vasculature, Cell **180**, 780 (2020).